Journal of Multidisciplinary Engineering Science and Technology (JMEST)
ISSN: 2458-9403
Vol. 4 Issue 6, June - 2017

Robust Adaptive Nonlinear Steering Control for Unmanned Rover Vehicle

Muhammad Adil, Aasma Abbas, Arsalan Abbas, Kashaf Basharat
Department of Electrical Engineering, COMSATS Institute of Information Technology
Wah 47040, Pakistan.
alishahbaz@ciitwah.edu.pk

***Abstract*—An unmanned rover vehicle is a surface creeping robot with many practical applications and it also acts as a testbed for simulation and verification of control algorithms. The control of steering dynamics of an unmanned rover using nonlinear adaptive control method has been considered. The system parameters are assumed unknown and the technique of nonlinear adaptation using manifold immersion is performed for their estimation. Reference tracking is obtained. The experimental validation of the theoretically proposed controller is presented by implementing discrete time realization of control algorithm using digital controller interfaced in real time with Simulink. The potential of proposed algorithm relies upon the flexibility in the structure of control algorithm and promising transient behavior of closed loop system dynamics.**

Keywords—unmanned rover vehicle; adaptive control; robust control; rapid control prototyping; parameter estimation

I. INTRODUCTION

An Unmanned Rover Vehicle (URV) or Autonomous Surface Vehicle (ASV) is a rover vehicle that lies in the domain of Remotely Operated Vehicles (ROV) running on land. It has various commercial applications as well as military uses. It has no crew so it presents many advantages in military applications and dangerous or tedious environmental conditions by reducing risk of loss of human life and time saving. They can be deployed to perform tasks such as mine counter measures, surveillance and reconnaissance, anti-warfare, fast on land attack robot, combat training, oil and gas exploration and construction, terrain data collection and environmental surveys.

There is a boom in the development of URV over past few decades. The unpredictable environmental conditions and complex dynamics of URVs make them a challenging system to be modelled and controlled. It also acts as a benchmark to simulate and test new and advanced control techniques. A mini URV has nonlinear dynamics. Moreover, by involving dynamics of the driving motor actuator along with the motor amplifier, complicates the problem still more as it adds more state variables in system dynamics, which tantamount to increase in the order of the system. To add to the difficulty, there are various uncertain system parameters. Hence there is always a room for a better and effective control technique for URV robot.

There are various control techniques available in literature. Control of a passively steered rover using 3-D kinematics is presented in [1], which considers differential wheel velocities for motion control. Motion planning and stochastic control with experimental validation on a planetary rover is presented in [2]. Trajectory tracking control of the Lunar Rover is investigated in [3], which focuses on a real Lunar rover trajectory tracking case, with respect to the sampling interference, transmission delay and energy limitation, a control-sampling co-design approach based on quadric optimal control is detailed. Research on intuitive controlling of unmanned Lunar Rover is presented in [4]. Path-tracking in URV is accomplished using feedback control of the position and orientation errors, measured with respect to the planned path trajectory in [5]. Online trajectory optimization using receding horizon guidance control for rovers is presented in [6], which is developed for guidance control with the real-time trajectory optimization. Dynamical reduction and output-tracking control of the Lunar Exploration Light Rover is presented in [7] with dynamical equations reduction using the Chaplygin reduction of nonholonomic systems. An artificial immune system for fault tolerant control of an over-actuated rover is considered in [8].

Most of these techniques consider the linear system model or a reduced order model of the system. Moreover, controllers do not have many tenable parameters to gain much control over system responses. Many controllers suffer degradation of response as the operation conditions change or the system parameters vary with time. We have applied a robust adaptive nonlinear control algorithm that relies on robustification of reduced order system controller against full order system dynamics [11]. The controller is also robust against unknow system parameters and has a lot of free tenable parameters to gain control over feedback dynamic response of the system output.

II. HARDWARE OVERVIEW

The hardware of rover vehicle is shown in Fig. 1. It consists of two DC motor driven vehicle carrying belts. DC motors have gear heads that increase the torque and payload carrying capacity of the rover. GPS and IMU sensors provide measurements. Rover has a data transceiver along with a camera transmitter for connection with the ground station as it will further be elaborated in the coming sections. The driving belts provide two forces on the rover platform producing counter torques, which producing steering manoeuvre of the rover as shown in Fig. 2. The control problem is to track the yaw angle of the vehicle, as measured by

the sensors, by manipulating the speeds of the two drive motors.

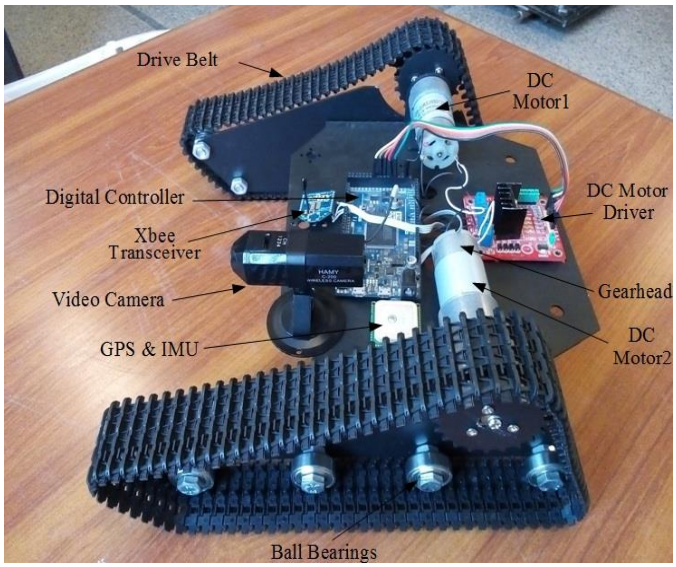

Fig. 1 *Rover hardware.*

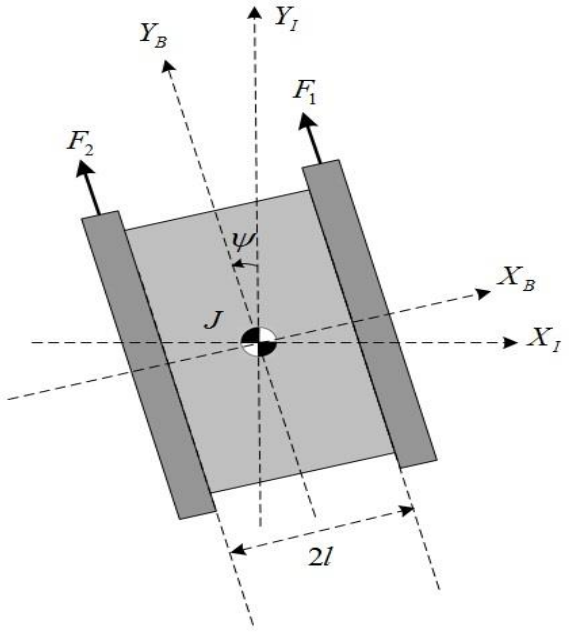

Fig. 2. *Rover control problem formulation.*

III. The Control Algorithm Synthesis

Consider a nonlinear parameter uncertain system,

$$\dot{\underline{p}} = \underline{s}\left(\underline{p}, u_e\right) = \underline{f}\left(\underline{p}\right) + \underline{g}\left(\underline{p}\right)u_e \qquad (1)$$

where $\underline{p} \in \mathbb{R}^n$ and $u_e \in \mathbb{R}^m$. The state vector $\underline{p}$ evolves on a smooth manifold P of dimension n, which is spanned by tangential manifold to the system map $\underline{s}$. The system map $\underline{s}$ in (1) has been decomposed into a drift vector field $\underline{f}(.)$ and a controlled vector field $\underline{g}$. In (1), $u_e \in U\left(\underline{p}\right)$ is the system forcing function with U a state dependent input set which belongs to the control bundle $\bigcup_{\underline{p}\in \mathrm{P}} U\left(\underline{p}\right)$. The topological manifold immersion based nonlinear control approach involves defining a reduced order exosystem. The state trajectories of the exosystem evolve on a C^∞ submanifold $\mathrm{Q} \subset \mathrm{P}$. The problem of controller design then boiled down to synthesize a control law that dynamically immerses the state trajectories of full order system to the manifold Q. Let us consider an exosystem with state vector $\underline{q} \in \mathbb{R}^q$ with $q < n$, which contains origin in its reachable set. This can be achieved by defining the vector field $\underline{\Upsilon}\left(\underline{q}\right)$ of the exosystem that governs the evolution of $\underline{q}$ as given by (2).

$$\dot{\underline{q}} = \underline{\Upsilon}\left(\underline{q}\right) \qquad (2)$$

Defining a smooth submanifold for the exosystem of (2) as:

$$\mathrm{Q} = \left\{\underline{p} \in \mathbb{R}^n \,\middle|\, \underline{p} = \underline{\psi}\left(\underline{q}\right); \underline{q} \in \mathbb{R}^q\right\} \qquad (3)$$

The controlled integral curves of system map $\underline{s}$ can be attracted by the submanifold Q if partial differential (4) along with the condition in (5) is satisfied [9].

$$\underline{f}\left(\underline{\psi}\left(\underline{q}\right)\right) + \underline{g}\left(\underline{\psi}\left(\underline{q}\right)\right)\wp\left(\underline{\psi}\right) = L_{\Upsilon}\underline{\psi} \qquad (4)$$

$$\underline{q}(t) = \underline{0} \quad \forall \ \underline{q}(0) \in \mathbb{R}^2 \text{ as } t \to \infty \qquad (5)$$

Here $L_{\underline{\Upsilon}}\underline{\psi} = (\nabla_{\underline{q}}\underline{\psi})\underline{\Upsilon}\left(\underline{q}\right)$ is the so-called Lie derivative. Also $\wp\left(\underline{\psi}\left(\underline{q}\right)\right) = v\left(\underline{\psi}\left(\underline{q}\right), 0\right)$ on the submanifold Q and $u = v\left(\underline{p}, \zeta\left(\underline{p}\right)\right)$ is the synthesized feedback control law that renders Q attractive. $\zeta(.)$ is the implicit description of Q and it is given by parameterized form in (6).

$$\zeta\left(\underline{p}\right) = \underline{p} - \underline{\psi}\left(\underline{q}\right) = 0 \qquad (6)$$

Introducing state variable $\hbar$ to define "off" the submanifold Q dynamics given by:

$$\dot{\hbar} = L_{\underline{s}}\zeta\Big|_{u=\vartheta\left(\underline{p},\hbar\right)} = \left(\frac{\partial\zeta}{\partial\underline{q}}\right)\underline{s}\left(\underline{p}, \vartheta\left(\underline{p}, \hbar\right)\right) \qquad (7)$$

In terms of $\hbar$ and any constant $\alpha > 0$, the synthesized controller ϑ the system mapping is given by,

$$\dot{\underline{p}} = \underline{s}\left(\underline{p}, \vartheta\left(\underline{p}, \hbar\right)\right) \qquad (8)$$

For any general system of form,

$$\begin{aligned} \dot{\underline{p}}_1 &= \underline{\xi}_1(p_1) + \underline{\xi}_2(\underline{p}_1)p_2 \\ \dot{p}_2 &= \underline{\varphi}(\underline{p})^T \underline{\lambda}_1 + \lambda_2 u \end{aligned} \qquad (9)$$

where $\underline{\xi}_1(.)$ and $\underline{\varphi}(.)$ are smooth mappings, λ_i are unknown parameters and $\dot{\underline{p}}_1 = \underline{\xi}_1(\underline{p}_1)$ is globally stable, then for constants $\varepsilon > 0$ and $k > 0$, the geometric adaptive estimates of λ_i are given by [9].

$$\dot{\underline{\hat{\lambda}}} = -\left(I + \nabla_{\underline{\hat{\lambda}}}\underline{\upsilon}\right)^{-1}\begin{pmatrix}\left(\nabla_{\underline{p}}\underline{\upsilon}\right)\left(\underline{\xi}_1(\underline{p}_1) + \underline{\xi}_2(\underline{p}_1)p_2\right)\\ +\dfrac{\partial \underline{\upsilon}}{\partial p_2}\left(-kp_2 - \varepsilon L_{\underline{\xi}}V_1(\underline{p}_1)\right)\end{pmatrix} \quad (10)$$

and the corresponding geomantic synthesized control law is given by,

$$u = -\left(\hat{\lambda}_2 + \upsilon_2(\underline{p}, \hat{\underline{\lambda}}_1)\right)\begin{pmatrix}kp_2 + \varepsilon L_{\underline{\xi}}V_1(\underline{p}_1)\\ +\varphi(\underline{p})^{\mathrm{T}}\left(\hat{\underline{\lambda}}_1 + \underline{\upsilon}_1(\underline{p})\right)\end{pmatrix} \quad (11)$$

The vector $\underline{\upsilon} = \left[\underline{\upsilon}_1(\underline{p}) \quad \upsilon_2(\underline{p}, \hat{\underline{\lambda}}_1)\right]^{\mathrm{T}}$ is given by:

$$\underline{\upsilon}_1(\underline{p}) = \gamma_1\int_0^{p_2}\varphi(\underline{p}_1, \eta)d\eta \quad (12)$$

$$\begin{aligned}\upsilon_2(\underline{p}, \hat{\underline{\lambda}}_1) &= \gamma_2\left(k\frac{p_2}{2} + \varepsilon L_{\underline{\xi}}V_1(\underline{p}_1)p_2\right)\\ &+ \gamma_2\int_0^{p_2}\varphi(\underline{p}_1, \eta)^{\mathrm{T}}\left(\hat{\underline{\lambda}}_1 + \underline{\upsilon}_1(\underline{p}_1, \eta)\right)d\eta\end{aligned} \quad (13)$$

Here $V_1(\underline{p}_1)$ is any mapping such that for some class-K function $\kappa(.)$, we have,

$$L_{\underline{\xi}}V_1(\underline{p}_1) \le -\kappa(\underline{p}_1) \quad (14)$$

and $\gamma_1 > 0$, $\gamma_2 > 0$ are constants [9].

IV. Systems Dynamics and Control

Consider the Rover in the Fig. 2. If ψ denotes yaw rover body rod and ω denotes the yaw rate then the system state variables for yaw dynamics are described by (15).

$$\underline{p} = \left[p_1 \quad p_2 \quad p_3\right]^{\mathrm{T}} = \left[\psi \quad \dot{\psi} \quad \omega\right]^{\mathrm{T}} \quad (15)$$

The system dynamics are given by,

$$\begin{aligned}\underline{f}(\underline{p}) &= \left[p_2 \quad -k_1p_2 + k_2p_3^2 \quad -p_3k_3\right]^{\mathrm{T}}\\ \underline{g}(\underline{p}) &= \left[0 \quad 0 \quad k_4\right]^{\mathrm{T}}\\ \underline{s}(\underline{p}, u_e) &= \left[p_3 \quad -k_1p_2 + k_2p_3^2 \quad -p_3k_3 + k_4u_e\right]^{\mathrm{T}}\end{aligned} \quad (16)$$

Now (2) and (8) evaluate to following expressions.

$$\underline{\Upsilon}(\underline{q}) = \left[q_2 \quad -k_1 + k_2\varsigma_1^2\right]^{\mathrm{T}} \quad (17)$$

$$\underline{p} = \underline{\psi}(\underline{q}) = \left[q_1 \quad q_2 \quad \psi_1(q_1, q_2)\right]^{\mathrm{T}} \quad (18)$$

$$\vartheta(\underline{p}, \hbar) = \left(-\alpha\hbar + \dot{\varsigma}_1 + k_3p_3\right)/k_4 \quad (19)$$

The reduced order system is given by (20).

$$\begin{aligned}\dot{\hbar} &= -\alpha\hbar\\ \dot{p}_1 &= p_2\\ \dot{p}_2 &= -k_1p_2 + k_2\varsigma_1^2\\ \dot{p}_3 &= -\alpha\hbar + \dot{\varsigma}_1\end{aligned} \quad (20)$$

The system in (20) immerses to system described by (21).

$$\begin{aligned}\dot{p}_1 &= p_2\\ \dot{p}_2 &= -k_1 + k_2\varsigma_1^2\end{aligned} \quad (21)$$

Let us consider feedback linearization of (21) as,

$$\varsigma_1 = \sqrt{u} : u > 0 \quad (22)$$

The immersion control law is given by,

$$\vartheta(\underline{p}, \hbar) = \frac{-\alpha\hbar + \dot{\varsigma}_1 + k_3p_3}{k_4} \quad (23)$$

Using (21) and (22) we get,

$$\dot{\underline{p}} = \left[p_2 \quad -k_1p_2 + k_2u\right]^{\mathrm{T}} \quad (24)$$

For the estimation of unknown parameters in (24), using the results in (9) through (14), we get.

$$\begin{aligned}&\underline{\xi}_1(p_1) = 0, \quad \underline{\xi}_2(\underline{p}_1) = 1,\\ &\lambda_1 = k_1, \quad \lambda_2 = k_2 > 0, \quad \varphi(\underline{p}) = -1\end{aligned} \quad (25)$$

$$L_{\underline{\xi}}V_1(\underline{p}_1) = 2\underline{p}_1 \quad (26)$$

$$\underline{\upsilon} = \begin{bmatrix}c_1p_2\\ c_2p_2^2 +_1 c_3\hat{\lambda}_1p_2 + c_4p_1p_2\end{bmatrix} \quad (27)$$

$$\nabla_{\hat{\underline{\lambda}}}\underline{\upsilon} = \begin{bmatrix}0 & 0\\ -\gamma_2p_2 & 0\end{bmatrix} \quad (28)$$

$$\nabla_{\underline{p}}\underline{\upsilon} = \frac{\partial \underline{\upsilon}}{\partial p_1} = \left[0 \quad 2\varepsilon\gamma_2p_2\right]^{\mathrm{T}} \quad (29)$$

$$\frac{\partial \underline{\upsilon}}{\partial p_2} = \left[-\gamma_1 \quad k\gamma_2p_2 + 2\gamma_2kp_1 - \gamma_2\hat{\lambda}_1 + \gamma_1\gamma_2p_2\right]^{\mathrm{T}} \quad (30)$$

The parameter estimates in (10) leads us to,

$$\dot{\underline{\hat{\lambda}}} = \begin{bmatrix}c_5p_1 + c_6p_2\\ c_7p_1^2 + c_8p_2^2 + c_9p_1p_2 + c_{10}p_2\hat{\lambda}_1 + c_{11}p_1\hat{\lambda}_1\end{bmatrix} \quad (31)$$

The control law in terms of estimates parameters is given by,

$$u = -\left(\hat{\lambda}_2 + \upsilon_2(\underline{p}, \hat{\underline{\lambda}}_1)\right)\left(kp_2 + 2\varepsilon p_1 - \hat{\underline{\lambda}}_1 - \underline{\upsilon}_1(\underline{p})\right) \quad (32)$$

At the last the reference tracking is achieved by modifications of control law as,

$$\vartheta'(\underline{p}, \hbar) = \frac{-\alpha\hbar + \dot{\varsigma}_1 + k_3p_3}{k_4} + \sigma(t) \quad (33)$$

A typical classical proportional derivative tracker law can be used to follow reference command as given by,

$$\sigma(t) = \Xi(e(t)) \quad (34)$$

$$\Xi(.) = -\frac{k_3}{k_4}\left(k_p(.) + k_d\frac{d(.)}{dt}\right) \quad (35)$$

The control law in (33) can be split to produce drive signals of two motors according to the splitter algorithm given by (36).

$$\vartheta_1 = \begin{cases} \left|\vartheta' - \vartheta'_m\right| + \vartheta_{1_{th}} & if \quad \left(\vartheta' - \vartheta'_m\right) > 0 \\ \vartheta_{1_{th}} & if \quad \left(\vartheta' - \vartheta'_m\right) < 0 \end{cases}$$
$$\vartheta_2 = \begin{cases} \left|\vartheta' - \vartheta'_m\right| + \vartheta_{2_{th}} & if \quad \left(\vartheta' - \vartheta'_m\right) < 0 \\ \vartheta_{2_{th}} & if \quad \left(\vartheta' - \vartheta'_m\right) > 0 \end{cases} \quad (36)$$

Here, $\vartheta_{i_{th}}$ is the upper threshold value of i^{th} motor drive signal dead zone and ϑ'_m is the mean value of signal ϑ'.

V. Sumulation and Testing

The values of various system parameters are given in Table 1. Using these values, the closed loop system is simulated in Fig. 3. The simulation result for yaw reference tracking response is shown in Fig. 4.

TABLE I. System Parameter Values

Parameter	Value	Parameter	Value
k_3	145	c_4	0.018
k_4	7.15	c_5	-0.25
k	61	c_6	-214
γ_1	4.1	c_7	5×10^{-4}
γ_2	1.0	c_8	845.0
ε	2.1×10^{-3}	c_9	0.25
c_1	-6.25	c_{10}	-750.0
c_2	72.0	c_{11}	-0.05
c_3	-3.25	c_{12}	0.125

The yaw response is stable with zero steady state error. The simulation result for the yaw rate response is shown in Fig. 5. The yaw rate decays to zero within 1.5 seconds. The simulation result for manipulated variables response is shown in Fig. 6. The magnitude of manipulated variables is within practical limits and drives the plant output to the desired reference signal.

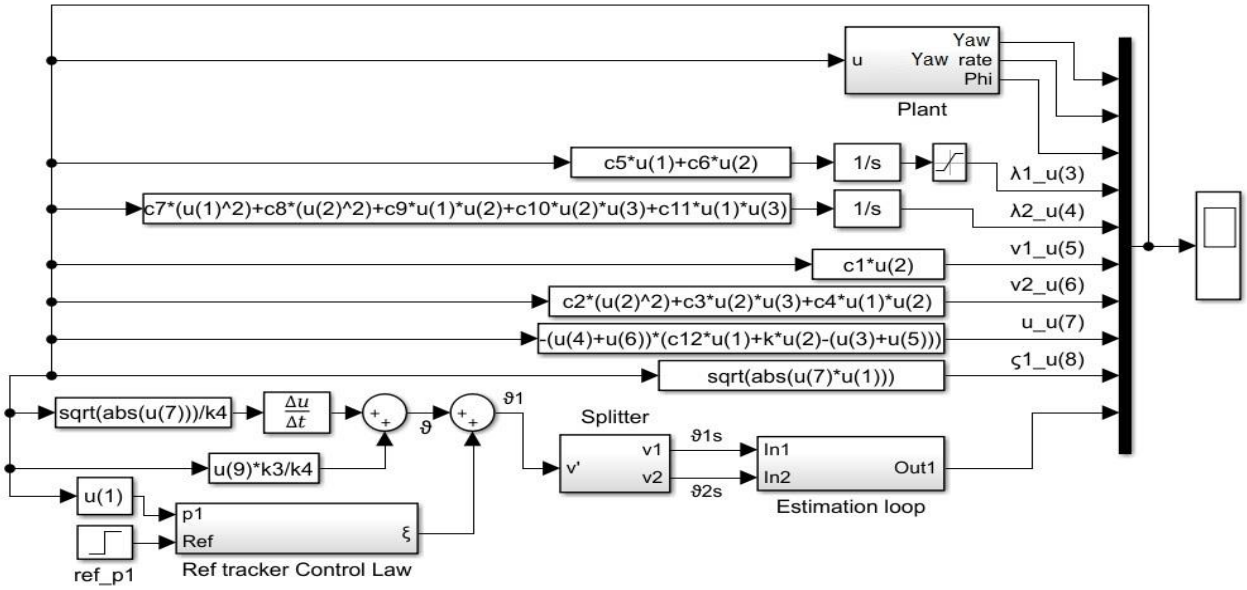

Fig. 3. *Simulation of system in MATLAB/Simulink*

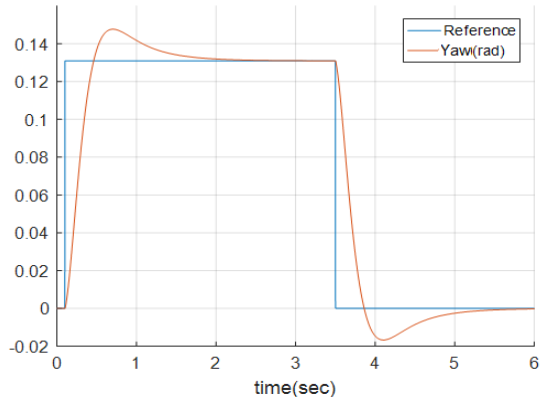

Fig. 4. *Yaw reference tracking.*

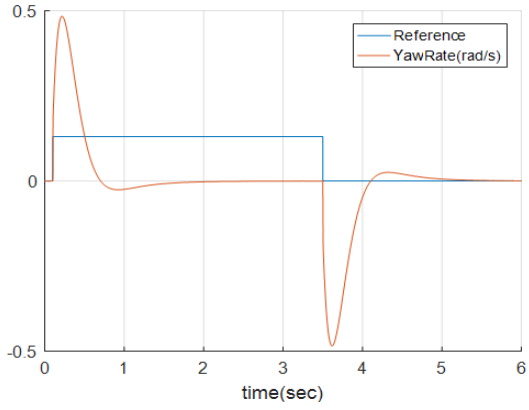

Fig. 5. *Yaw rate response.*

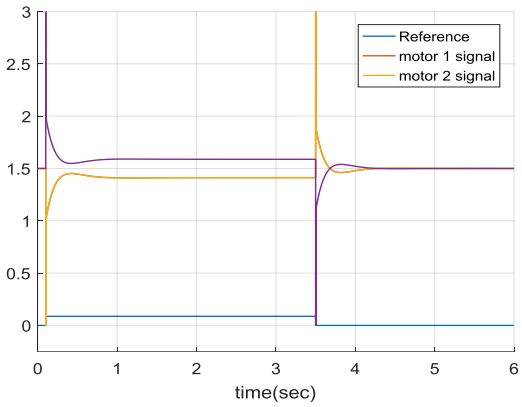

Fig. 6. *Manipulated variables' response.*

The experimental rapid control Prototyping (RCP) Simulink model of the closed loop system with reference tracker is shown in Fig. 7. The schematic representation of experimental hardware setup is shown in Fig. 8. It shows explicitly the components of the ground station as well as components of the URV. The complete experimental setup is shown in Fig. 9, which shows the components of ground station as well as that of unmanned rover vehicle.

The experimental result for yaw reference tracking response is shown in Fig. 10. Response of yaw rate variable is shown in Fig. 11. The Manipulated variables representing the magnitudes of drive signals of both gear headed DC motors driving the belts are shown in Fig. 12.

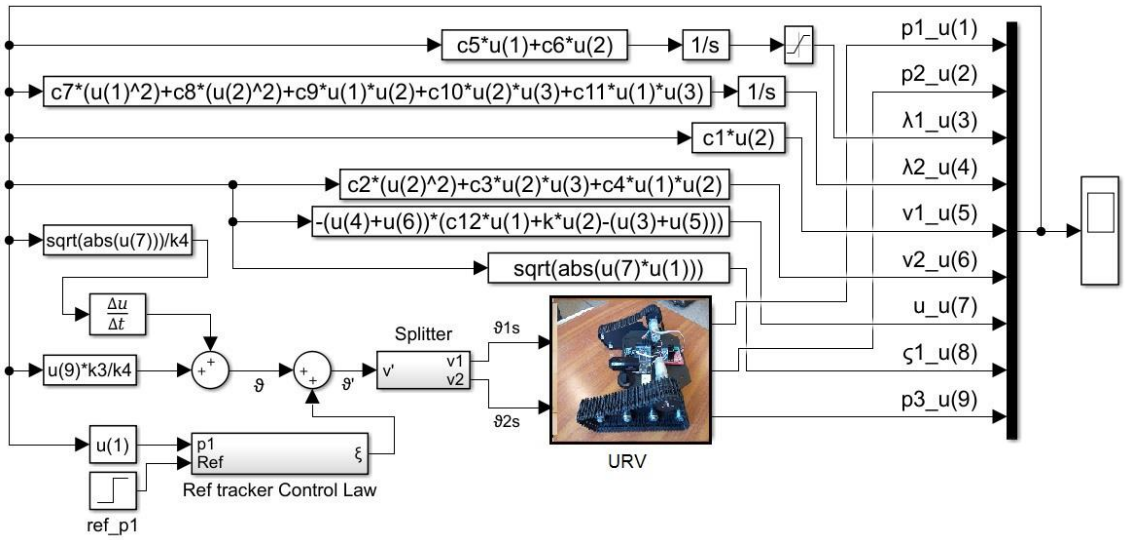

Fig. 7. *RCP Simulink model of the closed loop system.*

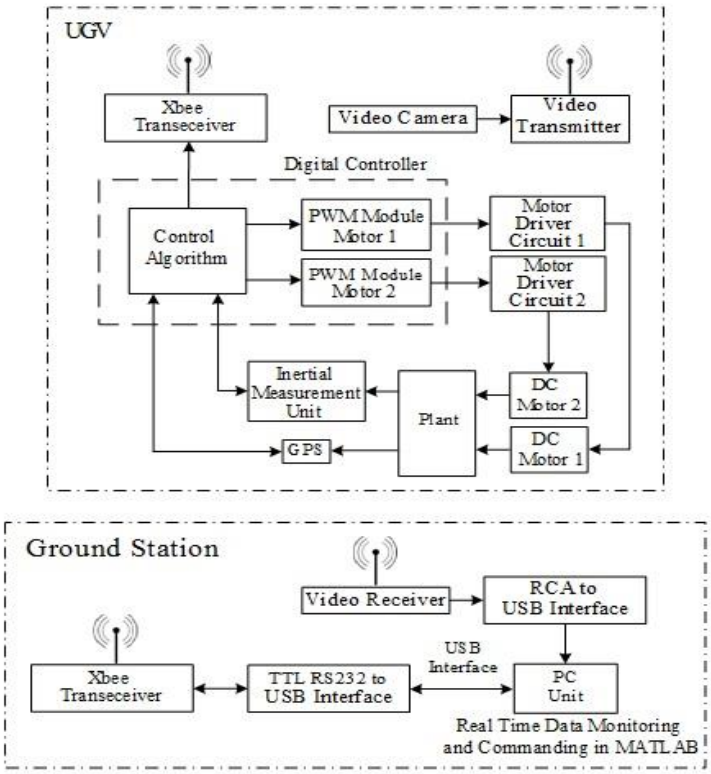

Fig. 8. *Schematic representation of experimental hardware setup.*

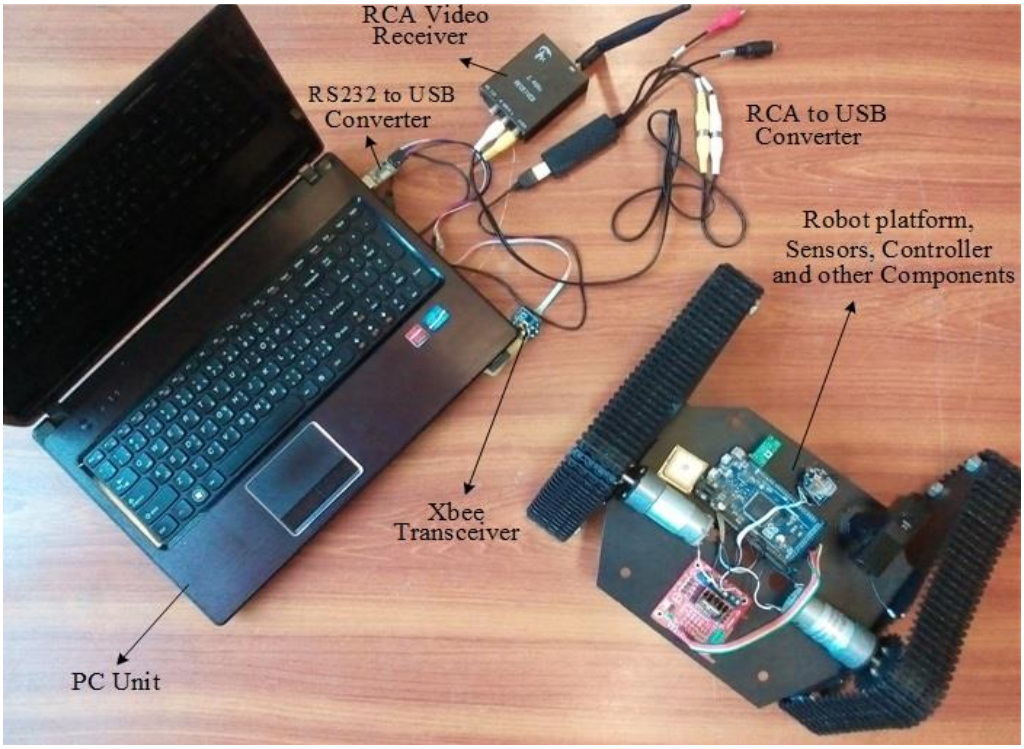

Fig. 9. *Complete experimental setup.*

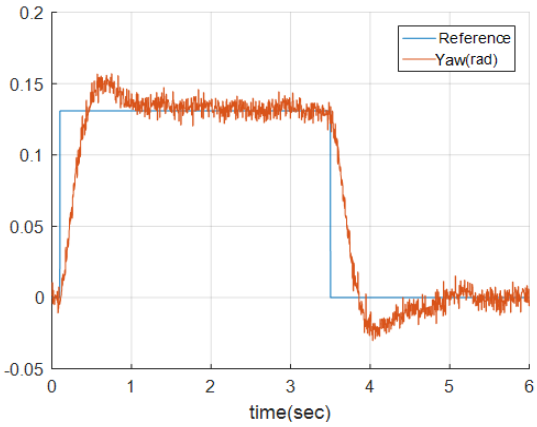

Fig. 10. *Experimental yaw reference tracking.*

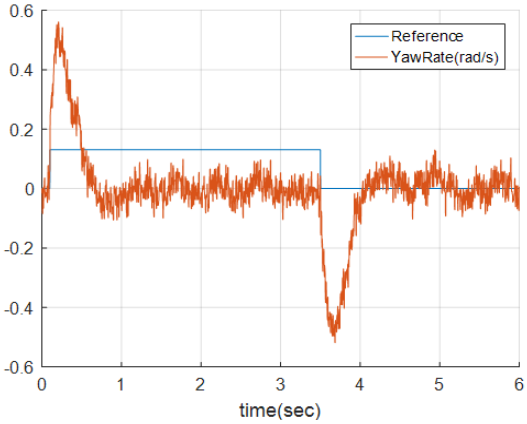

Fig. 11. *Experimental yaw rate response.*

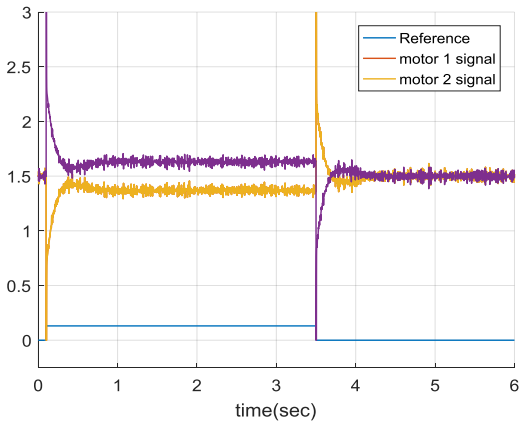

Fig. 12. *Experimental Manipulated variables' response.*

Yaw reference response is stable with zero steady state error in Fig. 10. The simulation result for the yaw rate response as shown in Fig. 11, decays to zero within 1.5 seconds. The simulation result for manipulated variables response as shown in Fig. 12, has magnitude of variables within practical limits and drives the plant output to the desired reference signal.

VI. CONCLUSIONS

A robust nonlinear adaptive controller for the yaw dynamics or steering of a mini URV has been presented. System parameters are considered unknown and they are estimated using nonlinear adaptation. The proposed control technique is simulating in Simulink. The theoretical technique is

tested in real time using digital controllers and data acquisition cards. The control algorithm has a lot of free tenable parameters. The results showed promising behavior of closed loop system in the presence of parameters uncertainties. Moreover, a greater control of closed loop system dynamics is possible owing to the flexibility in control algorithm.

REFERENCES

[1] N. Seegmiller and D. Wettergreen, "Control of a passively steered rover using 3-D kinematics," IEEE/RSJ International Conference on Intelligent Robots and Systems, San Francisco, CA, pp. 607-612, 2011.

[2] R. McAllister, T. Peynot, R. Fitch and S. Sukkarieh, "Motion planning and stochastic control with experimental validation on a planetary rover," IEEE/RSJ International Conference on Intelligent Robots and Systems, Vilamoura, pp. 4716-4723, 2012.

[3] Z. Yang and W. S. Yu, "Trajectory tracking control of the Lunar Rover," Proceedings of the 32nd Chinese Control Conference, Xi'an, pp. 2233-2239, 2013.

[4] Y. Cheng, Z. Jianliang, D. Yingli and Z. Wei, "Research on intuitive controlling of unmanned Lunar Rover," The 27th Chinese Control and Decision Conference (2015 CCDC), Qingdao, pp. 4917-4922, 2015.

[5] D. N. Green, J. Z. Sasiadek and G. S. Vukovich, "Guidance and control of an autonomous planetary rover," Vehicle Navigation and Information Systems Conference, 1993., Proceedings of the IEEE-IEE, Ottawa, Ontario, Canada, pp. 539-542, 1993.

[6] K. Shinomoto, T. Higuchi and D. Toratani, "Online trajectory optimization using receding horizon guidance control for rovers," IEEE/SICE International Symposium on System Integration (SII), Nagoya, 2015, pp. 977-982, 2015.

[7] R. Chhabra, "Dynamical reduction and output-tracking control of the Lunar Exploration Light Rover (LELR)," 2016 IEEE Aerospace Conference, Big Sky, MT, pp. 1-8, 2016.

[8] R. Kidd and C. Crane, "An artificial immune system for fault tolerant control of an over-actuated rover," 16th International Conference on Control, Automation and Systems (ICCAS), Gyeongju, pp. 388-391, 2016.

[9] A. Astolfi, and R. Ortega, “Immersion and invariance: a new tool for stabilization and adaptive control of nonlinear systems,” IEEE Transactions on Automatic Control, 48(4), pp. 590–606, 2003.